NANO · MICRO small
www.small-journal.com

Adsorption-Free Growth of Ultra-Thin Molybdenum Membranes with a Low-Symmetry Rectangular Lattice Structure

Jingjing Si, Mengqi Zeng, Huy Q. Ta, Shuting Zheng, Jihai Liao, Xiaobao Yang, Mark H. Rümmeli,* and Lei Fu**

Although low-symmetry lattice structure of 2D transition metals is highly anticipated for both fundamental research and potentially distinctive application, it still has not been experimentally realized, which greatly hinders the exploration of the unique properties. Here, ultra-thin body-centered-cubic (bcc) phase molybdenum (Mo) membranes are successfully synthesized with a low-symmetry rectangular (110) crystal face via an adsorption-free reaction. Through experimental and density functional theory studies, no foreign atoms being adsorbed is shown to be a key factor for the successful preparation of the bcc phase 2D transition metal with (110) faces. The realization of 2D Mo(110) with a low-symmetric rectangular lattice structure extends the scope of 2D structures and is also beneficial for the exploration and development of low-symmetry rectangular lattice-structured materials with unique properties.

2D transition metals have garnered tremendous interest due to their excellent performance in catalysis, magnetism, and superconductivity.[1,2] The physical and chemical properties of transition metals can be finely tuned depending on their preferentially exposed crystal face, which determines their surface atomic arrangement and coordination.[3–6] This makes them attractive for a range of applications. Thus, controlled synthesis of 2D transition metals with a particular lattice structure is important and will open up numerous opportunities to expand their functionalities and potential applications.

At present, many symmetric lattice structures have been prepared in 2D elementary nanosheets, and a few unusual low-symmetric structures have been reported due to the special arrangement of the structure. However, most of them are concentrated in the main group elements. A low-symmetry rectangular lattice structure can be observed perpendicular to the surface in black phosphorene, due to its particular puckered honeycomb structure.[7] 2D β_{12} boron (B) sheets have a low-symmetry rectangle lattice structure consisted of the periodically arranged atom clusters and vacancies.[8] These unique low-symmetry lattice structures would bring about some special physical or chemical properties. For example, it is promising for 2D β_{12} B sheets producing massless Dirac fermions.[8] To date, only 2D transition metals exposing supersymmetric lattice structures have been demonstrated, even some transition metals have a rectangular lattice structure on one of their crystal faces.[9–13] For example, the lattice structure of (110) crystal face of bcc phase transition metals is a centered

J. J. Si, Prof. M. Q. Zeng, S. T. Zheng, Prof. L. Fu
College of Chemistry and Molecular Sciences
Wuhan University
Wuhan 430072, China
E-mail: leifu@whu.edu

Dr. H. Q. Ta, Prof. M. H. Rümmeli
Soochow Institute for Energy and Materials Innovations
College of Physics
Optoelectronics and Energy
Collaborative Innovation Center of Suzhou
Nano Science and Technology
Key Laboratory of Advanced Carbon Materials
and Wearable Energy Technologies of Jiangsu Province
Soochow University
Suzhou 215006, China
E-mail: mhr1@suda.edu.cn

Dr. J. H. Liao, Prof. X. B. Yang
Department of Physics
South China University of Technology
Guangzhou 510640, China
E-mail: scxbyang@scut.edu.cn

Prof. M. H. Rümmeli
Centre of Polymer and Carbon Materials
Polish Academy of Sciences
M. Curie-Skłodowskiej 34, Zabrze 41–819, Poland

Prof. M. H. Rümmeli
Institute of Environmental Technology
VSB-Technical University of Ostrava
17. Listopadu 15, Ostrava 708 33, Czech Republic

Prof. L. Fu
The Institute for Advanced Studies
Wuhan University
Wuhan 430072, China

The ORCID identification number(s) for the author(s) of this article can be found under https://doi.org/10.1002/smll.202001325.

DOI: 10.1002/smll.202001325

low-symmetric rectangle.[14–16] Generally, 2D bcc phase transition metals with low index (110) faces exposed should be easy to obtain due to the lowest intrinsic surface energy. However, to date, no one has demonstrated 2D bcc phase transition metal with a (110) crystal face, which has a low-symmetric rectangular lattice structure. The reason for the difficulty of synthesis is not understood. Insight into this issue would shed light on the design of new materials with special atomic arrangement and facilitate their application in high-performance catalytic reactions and in devices.

Here, we have, for the first time, successfully synthesized ultra-thin molybdenum (Mo) membranes with a low-symmetric rectangular (110) crystal face via an adsorption-free reaction. This was achieved by the in situ electron-beam irradiation of 2D α-molybdenum carbide (α-Mo_2C) single crystals. Through experimental and theoretical investigations, we find that the lack of adsorbed foreign atoms can result in the formation of 2D Mo membranes with a rectangular (110) crystal face. In addition, density functional theory (DFT) studies reveal that the novel 2D Mo membrane is metallic and has a high density of d states at the Fermi level, which could be attractive for high-performance catalytic reactions and superconductivity.

In situ investigations using a spherical aberration-corrected transmission electron microscopy (ACTEM) were employed. The 2D α-Mo_2C single crystals were chosen as the starting material. Under electron-beam irradiation of 2D α-Mo_2C, because of its semi-metallic nature and the inclusion carbon (C) which is a light element, it is argued that the knock-on damage dominates over radiolysis as the driving mechanism for bond breakage in the 2D α-Mo_2C single crystals.[17–23] Sputtering enables the preferential removal of C to form defects in the 2D α-Mo_2C structure once the beam energy exceeds the knock-on damage threshold of the thin 2D α-Mo_2C (above 80 kV as discussed below) and the remaining Mo atoms rapidly rearrange to form Mo membranes. For example, by condensing an electron beam at selected regions of a 2D α-Mo_2C single crystal (200 kV, 5.5 nA), a distinct rectangular lattice structure appears which differs from the original α-Mo_2C hexagonal lattice (Figure S1, Supporting Information).[24] In addition, within the thin α-Mo_2C single crystal one can form vacancies/defects that can expand into relatively large holes in the irradiated regions with extended exposures (**Figure 1**a). The local energy-dispersive X-ray (EDX) spectrum shows the resulting rectangular lattice structure comprises 100% Mo (Figure 1b). The lattice constants of the observed rectangular lattice structure are 2.33 and 1.67 Å, and the corresponding Fourier-transformed image is also provided in the inset of Figure 1a. Image simulations show the structure fits that of ultra-thin AB stacked Mo(110) with even atom thickness (2, 4, etc.), which has a rectangular lattice structure (Figure 1c,d and Figure S2, Supporting Information). Form Figure 1d and Figure S2 in the Supporting Information, we can see the atoms in the second layer occupy in the center of the rhombus, and the stacking order is ABAB..., i.e., the third layer is exactly below the first one. The lattice constant for the AB stacked Mo(110) is ≈3.30 Å from the experimental data, which is larger than that of the bulk bcc Mo (3.14 Å). We attribute this to the lattice dilation due to the low dimensions of the Mo membranes, similar to the case found with 2D Fe membranes.[25] The thickness of Mo

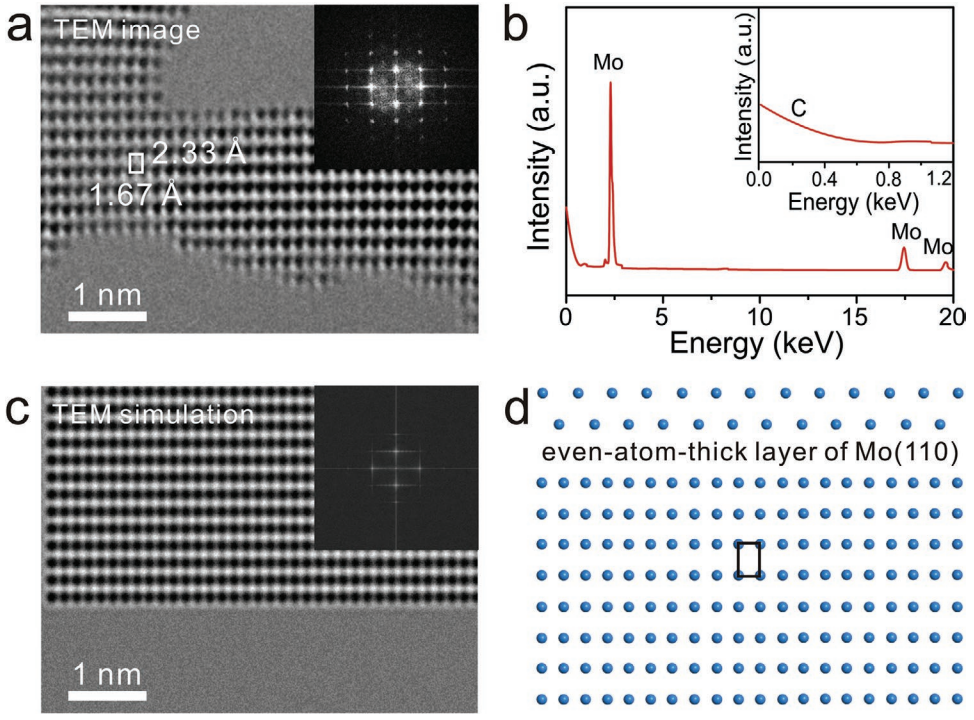

Figure 1. Characterization of free-standing ultra-thin Mo membrane with a low-symmetry rectangular lattice structure. a) The TEM image of the rectangular lattice structure of ultra-thin Mo membrane. The inset shows the corresponding Fourier-transformed image. b) EDX spectra of ultra-thin membrane after the electron-beam irradiation in micro-region. c) Simulated TEM image of two-atom-thick layer of Mo(110). The inset shows the corresponding Fourier-transformed image. d) Image simulations of even-atom-thick layer of Mo(110).

has a correlation with that of the precursor material (α-Mo_2C) (Figure S3, Supporting Information). Figure S4 in the Supporting Information shows the sequential time-dependent TEM images of the structural transformation from 2D α-Mo_2C to 2D Mo under 200 kV electron irradiation. Under the beam irradiation, vacancies/defects are created in the 2D α-Mo_2C single crystal. After 360 s irradiation, the vacancies/defects extended into holes with diameters of 0.6–1 nm as shown in Figure S4b (Supporting Information). Simultaneously, we can observe Mo atoms rearranging to form a rectangular lattice structure over time (Figure S4b–d, Supporting Information). Under the continuous irradiation of the external electron beam, the sputtered C atoms will continuously enter the vacuum of the microscope, which will not be absorbed during the radiolysis of α-Mo_2C. To better understand the formation of the 2D Mo membranes, we explored different electron-beam irradiation energies using acceleration voltages of 80, 200, and 300 kV. The conversion of α-Mo_2C to Mo(110) occurred at 200 and 300 kV but was not observed at 80 kV and this strongly suggests that knock-on damage dominates over radiolysis as the driving mechanism for bond breakage in the 2D α-Mo_2C single crystal. Sputtering enables the preferential removal of C atoms to form defects in the 2D α-Mo_2C, once the electron beam energy exceeds the knock-on damage threshold (somewhere above 80 kV), and the remaining Mo atoms rapidly rearrange to form Mo membranes.

An interesting question is why (100) crystal faces are generally reported in the literature rather than (110) faces in 2D bcc transition metal since the (110) crystal faces have the lowest surface energy.[9] Generally, a clean surface that is not stable can more easily adsorb foreign atoms, e.g., such as common contaminants like C and oxygen (O) atoms, making it more stable, owing to having relatively more unsaturated bonds. Considering that our obtained ultra-thin Mo membranes with intrinsic low surface energy (110) face show no contamination in our experiment, we inferred that controlling the adsorption of foreign atoms is essential for the synthesis of 2D bcc phase metal with intrinsic low surface energy (110) faces exposed. To verify this, further experiments in which we deliberately introduced randomly distributed adsorbents were conducted. We exposed the rectangular structured Mo membranes to air. We found that the rectangular structure of ultra-thin Mo disappeared and transformed to an amorphous film with the existence of C and O (Figure S5 and Table S1, Supporting Information). After exposure to the atmosphere, the samples were reinserted to the TEM and exposed to an electron beam. The majority of the regions comprising amorphous Mo crystallized with a symmetrical square lattice structure while only a few regions crystallized with a low-symmetry rectangular lattice structure (**Figure 2**a). Image simulations correspond with Mo(100) (Figure S6, Supporting Information). Local EDX spectrum of recrystallized amorphous Mo shows that the signal of O disappears while the signal of C remains (Table S2, Supporting Information), suggesting that the formation of the (100) face is resulted from the presence of C in this process. To further test the effect of C, we used a 2D α-Mo_2C/graphene vertical heterojunction as the starting material in order to make sure that C adsorption was kept in the irradiation process. After that the samples were exposed to the electron-beam irradiation and the C atoms in the 2D α-Mo_2C were removed, for the obtained

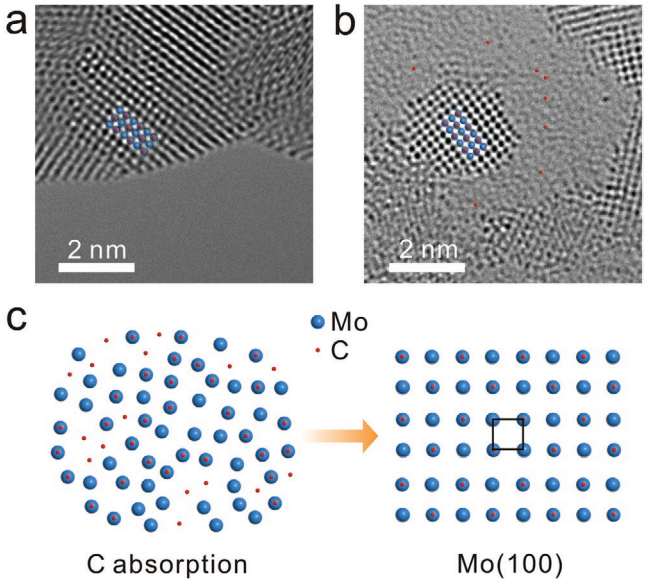

Figure 2. Characterization of 2D Mo membrane with a symmetrical square lattice structure. a) The TEM image of 2D Mo membrane with a symmetrical square lattice structure derived from the re-crystallized amorphous Mo with C and O adsorption after the electron-beam irradiation. b) The TEM image of 2D Mo membrane with a symmetrical square lattice structure derived from the 2D α-Mo_2C/graphene vertical heterojunction after the electron-beam irradiation. c) A schematic diagram for the formation of 2D Mo membrane with a symmetrical (100) square lattice structure via the C adsorption (blue solid circles represent Mo atoms, and red solid circles represent C atoms).

2D Mo, the majority of the regions exhibited a symmetrical square lattice while only a few regions appeared with the low-symmetry rectangular lattice structure (Figure 2b). Here, we also employed the theoretical calculations to verify the impact of C and O adsorption on the total energy of three low index faces of 2D bcc Mo, including (100), (110), and (111). The first-principles calculations were based on DFT using the Vienna ab initio simulation package (VASP). The calculation results show that the total energies of three clean low (100), (110), and (111) faces of 2D bcc Mo are −10.451, −10.640, and −10.134 eV, respectively (**Figure 3**), corresponding to cohesive energies of 5.863, 6.052, and 5.546 eV, respectively (Table S3, Supporting Information). Furthermore, it is worth pointing out that the adsorption of C and O on (100), (110), and (111) surface is a spontaneous exothermic process. The (100) faces tend more likely to adsorb C atoms than O atoms as they release more energy. The impact of C and O adsorption on the total energy of the three low index (100), (110), and (111) faces is plotted in Figure 3 and Figure S7, Supporting Information. After the adsorption of C or O, the (100) face has the lowest energy, followed by the (110) face, and finally the (111) face. This explains the reason why the majority of the regions in Mo possesses a (100) face with a symmetrical square lattice structure when using the re-irradiated amorphous Mo with C and O adsorption, and the 2D α-Mo_2C/graphene vertical heterojunction as the starting material under an electron beam. A schematic diagram for the formation of 2D Mo membranes with symmetrical (100) square lattice structure is shown in Figure 2c. Therefore, based on the experiments and theoretical calculations, we can infer that the impact of foreign

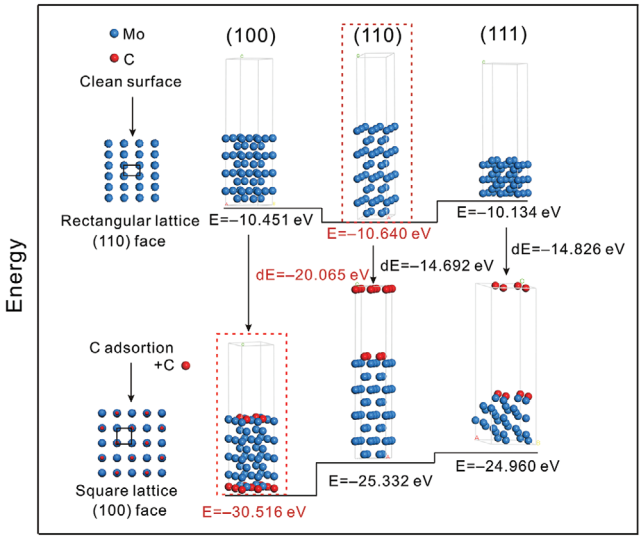

Figure 3. The impact of C adsorption on total energies of three low index (100), (110), and (111) faces of 2D bcc Mo, respectively.

atom adsorption (e.g., C, O, or other foreign atoms) during the preparation of 2D bcc phase transition metals results in the exposure of (100) crystal face. Therefore, no adsorption of foreign atoms is a key factor for the successful preparation of bcc phase 2D transition metal with a (110) exposed face.

Finally, we examined the phonon dispersion spectra and band structure of the ultra-thin Mo membrane as a new 2D crystal in order to elucidate its nature in terms of the stability and electronic structure. The phonon spectra show that there is no imaginary frequency for free-standing ultra-thin Mo(110) membranes (2, 4, 6 atom thickness) (**Figure 4**a and Figure S8 in the Supporting Information). Thus, the (110) crystal face of the bcc phase is stable and this is consistent with our experimental results of 100% pure ultra-thin Mo(110) membrane with intrinsic low surface energy. The band structure and partial density of states (PDOS) of the ultra-thin Mo(110) membrane are shown in Figure 4b,c and Figures S9 and S10 in the Supporting Information. They reveal that the ultra-thin Mo membranes are metallic and own a large number of d states near the Fermi level, which could be utilized for catalytic reactions or superconductivity. When the number of Mo layers is reduced to 2, 4, 6 atomic layers, one can see that it approximates duple d states near the Fermi level relative to the bulk bcc Mo, indicating that the catalytic performance will be greatly improved (Figure 4c and Figure S10, Supporting Information).

In conclusion, we have reported ultra-thin Mo membranes with a low-symmetry rectangular (110) crystal face via an adsorption-free reaction for the first time. The DFT studies reveal that the novel ultra-thin Mo membranes are metallic and have a high density of d states at the Fermi level, which could be attractive for catalytic reactions or superconductivity. Remarkably, the ultra-thin Mo membranes have a low-symmetry rectangular lattice, which undoubtedly broadens the family of 2D materials as well as the unique physical and chemical properties of such materials. Furthermore, through experimental and theoretical investigations, we demonstrated that no adsorption of foreign atoms (even the most common C and O) is a key factor for the successful preparation of bcc phase 2D transition metal with a (110) facet. We believe that these results will provide new insight for the preparation of well-defined 2D transition metals with (110) faces and also be beneficial for the exploration and development of low-symmetry rectangular lattice structured materials with unique properties.

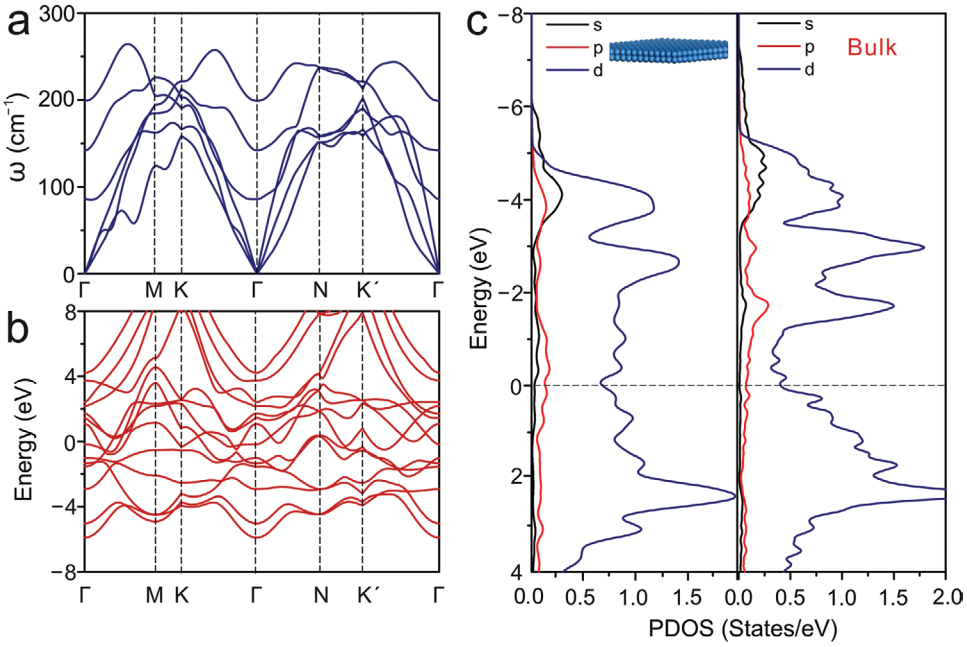

Figure 4. The electronic structures of the free-standing ultra-thin Mo(110) membrane with a low-symmetry rectangular lattice structure. a) Phonon band dispersions of two-atom-thick layer of Mo(110). b) The band structure of two-atom-thick layer of Mo(110). c) The PDOS of two-atom-thick layer of Mo(110) (left) and bcc bulk Mo (right).

Supporting Information

Supporting Information is available from the Wiley Online Library or from the author.

Acknowledgements

J.J.S., M.Q.Z., and H.Q.T. contributed equally to this work. The research was supported by the National Natural Science Foundation of China (Grant 21673161, 21905210, 21991154), the Czech Republic from ERDF "Institute of Environmental Technology – Excellent Research" (No. CZ .02.1.01/0.0/0.0/16_019/0000853), and the Sino-German Center for Research Promotion (Grant GZ 1400).

Conflict of Interest

The authors declare no conflict of interest.

Keywords

2D materials, heterogenous adsorption, low symmetry, molybdenum, rectangular lattice structure

Received: February 29, 2020
Revised: April 22, 2020
Published online: June 2, 2020

[1] X. Kong, Q. Liu, C. Zhang, Z. Peng, Q. Chen, *Chem. Soc. Rev.* **2017**, *46*, 2127.
[2] L. Lin, B. Deng, J. Sun, H. Peng, Z. Liu, *Chem. Rev.* **2018**, *118*, 9281.
[3] R. Long, K. Mao, X. Ye, W. Yan, Y. Huang, J. Wang, Y. Fu, X. Wang, X. Wu, Y. Xie, Y. Xiong, *J. Am. Chem. Soc.* **2013**, *135*, 3200.
[4] D. Lei, K. Yu, M.-R. Li, Y. Wang, Q. Wang, T. Liu, P. Liu, L.-L. Lou, G. Wang, S. Liu, *ACS Catal.* **2017**, *7*, 421.
[5] M. Zhao, Z. Chen, Z. Lyu, Z. D. Hood, M. Xie, M. Vara, M. Chi, Y. Xia, *J. Am. Chem. Soc.* **2019**, *141*, 7028.
[6] Y. Liu, H.-Y. Ma, D. Lei, L.-L. Lou, S. Liu, W. Zhou, G.-C. Wang, K. Yu, *ACS Catal.* **2019**, *9*, 8306.
[7] C. Wang, Q. He, U. Halim, Y. Liu, E. Zhu, Z. Lin, H. Xiao, X. Duan, Z. Feng, R. Cheng, N. O. Weiss, G. Ye, Y. C. Huang, H. Wu, H. C. Cheng, I. Shakir, L. Liao, X. Chen, W. A. Goddard III, Y. Huang, X. Duan, *Nature* **2018**, *555*, 231.
[8] B. Feng, J. Zhang, Q. Zhong, W. Li, S. Li, H. Li, P. Cheng, S. Meng, L. Chen, K. Wu, *Nat. Chem.* **2016**, *8*, 563.
[9] H. Liu, H. Tang, M. Fang, W. Si, Q. Zhang, Z. Huang, L. Gu, W. Pan, J. Yao, C. Nan, H. Wu, *Adv. Mater.* **2016**, *28*, 8170.
[10] H. Duan, N. Yan, R. Yu, C. R. Chang, G. Zhou, H. S. Hu, H. Rong, Z. Niu, J. Mao, H. Asakura, T. Tanaka, P. J. Dyson, J. Li, Y. Li, *Nat. Commun.* **2014**, *5*, 3093.
[11] X. Huang, S. Li, Y. Huang, S. Wu, X. Zhou, S. Li, C. L. Gan, F. Boey, C. A. Mirkin, H. Zhang, *Nat. Commun.* **2011**, *2*, 292.
[12] Y. Kuang, G. Feng, P. Li, Y. Bi, Y. Li, X. Sun, *Angew. Chem., Int. Ed.* **2016**, *55*, 693.
[13] S. Gao, Y. Lin, X. Jiao, Y. Sun, Q. Luo, W. Zhang, D. Li, J. Yang, Y. Xie, *Nature* **2016**, *529*, 68.
[14] M. J. Calhorda, R. Hoffmann, C. M. Friend, *J. Am. Chem. Soc.* **1990**, *112*, 50.
[15] T. Jirsak, J. A. Rodriguez, J. Hrbek, *Surf. Sci.* **1999**, *426*, 319.
[16] T. Jirsak, M. Kuhn, J. A. Rodriguez, *Surf. Sci.* **2000**, *457*, 254.
[17] R. F. Egerton, P. Li, M. Malac, *Micron* **2004**, *35*, 399.
[18] J. Lin, O. Cretu, W. Zhou, K. Suenaga, D. Prasai, K. I. Bolotin, N. T. Cuong, M. Otani, S. Okada, A. R. Lupini, J. C. Idrobo, D. Caudel, A. Burger, N. J. Ghimire, J. Yan, D. G. Mandrus, S. J. Pennycook, S. T. Pantelides, *Nat. Nanotechnol.* **2014**, *9*, 436.
[19] X. Zhao, J. Dan, J. Chen, Z. Ding, W. Zhou, K. P. Loh, S. J. Pennycook, *Adv. Mater.* **2018**, *30*, 1707281.
[20] J. Lin, S. T. Pantelides, W. Zhou, *ACS Nano* **2015**, *9*, 5189.
[21] X. Liu, T. Xu, X. Wu, Z. Zhang, J. Yu, H. Qiu, J. H. Hong, C. H. Jin, J. X. Li, X. R. Wang, L. T. Sun, W. Guo, *Nat. Commun.* **2013**, *4*, 1776.
[22] X. Huang, Z. Zeng, H. Zhang, *Chem. Soc. Rev.* **2013**, *42*, 1934.
[23] Z. Liu, Z. Fei, C. Xu, Y. Jiang, X. L. Ma, H. M. Cheng, W. Ren, *Nanoscale* **2017**, *9*, 7501.
[24] C. Xu, L. Wang, Z. Liu, L. Chen, J. Guo, N. Kang, X. L. Ma, H. M. Cheng, W. Ren, *Nat. Mater.* **2015**, *14*, 1135.
[25] J. Zhao, Q. Deng, A. Bachmatiuk, G. Sandeep, A. Popov, J. Eckert, M. H. Rümmeli, *Science* **2014**, *343*, 1228.